Journal of Materials Chemistry C

Accepted Manuscript

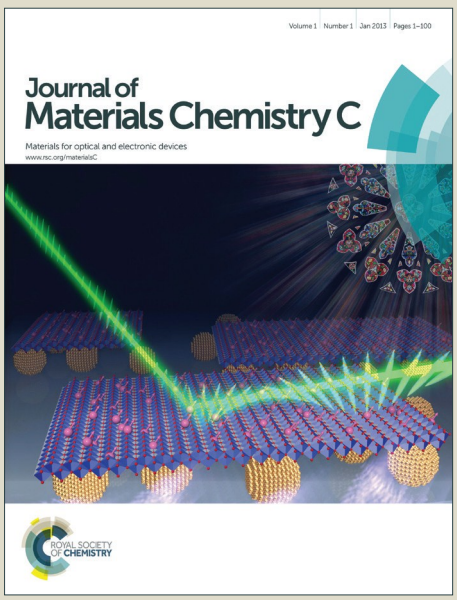

ROYAL SOCIETY OF CHEMISTRY

www.rsc.org/materialsC

Journal of Materials Chemistry C

Journal of Materials Chemistry C

Dynamic Article Links ►

Cite this: DOI: 10.1039/c0xx00000x

ARTICLE TYPE

www.rsc.org/xxxxxx

Substituent groups effect on the morphology and memory performance of phenazine derivatives

Pei-Yang Gu,[1] Yong Ma,[2] Jing-Hui He,[2] Guankui Long,[1] Chengyuan Wang,[1] Wangqiao Chen,[1] Yi Liu,[3] Qing-Feng Xu,[2,*] Jian-Mei Lu,[2,*] and Qichun Zhang[1,4*]

Received (in XXX, XXX) Xth XXXXXXXXX 20XX, Accepted Xth XXXXXXXXX 20XX
DOI: 10.1039/b000000x

In this paper, we focused on how the film morphology changes can affect the memory performance based on phenazine derivatives because the performance of many devices is strongly dependent on the morphology of organic molecules in the as-prepared films. To address this point, two phenazine derivatives, 7,8-bis(decyloxy)-3-(2-hydroxy-4,5-dinitrophenoxy)phenazin-2-ol (2OHPz) and 7,8-bis(decyloxy)-3-(2-(decyloxy)-4,5-dinitrophenoxy)phenazin-2-ol (1OHPz) have been successfully synthesized and characterized. The two compounds have the same electron-withdrawing groups (nitro and pyrazine) and molecular backbone, but different terminal substituted groups, which would be very helpful to allow us understand how substituted group to affect the morphology and device performance. In fact, the sandwich-structured memory devices based on ITO/2OHPz/Al exhibited excellent ternary memory behavior with high ON2/ON1/OFF current ratios of $10^{8.8}/10^{3}/1$ at switching threshold voltages of -1.80 V/-3.62 V while the memory devices based on ITO/1OHPz/Al displayed binary memory behavior with ON/OFF current ratios of $10^{7.5}/1$ at a switching threshold voltage of -3.0 V. The different memory behaviors are attributed to the different molecular packing in the two phenazine derivatives, which is confirmed by AFM, XRD and UV-vis absorption. The AFM height image of the 2OHPz film thermally evaporated onto the ITO surface indicates the formation of self-organized fibril structures, which is in sharp contrast to that of the 1OHPz film. This variation suggests different degrees of aggregation in these films, which is also in accordance with the XRD and UV-vis absorption results. There is one diffraction peak at 2^{-} 16.11° for the film of 2OHPz, indicating the formation of more ordered structure in the thin film. In contrast, there is no obvious diffraction peak in the film of 1OHPz. Moreover, the UV-vis absorption wavelength of 2OHPz at the thin film is blue-shifted ~ 10 nm more than that of 1OHPz film compared to those in dichloromethane.

1 Introduction

Recently, organic materials for high-density data storage have received increasing attention due to their tunable properties through modifying the molecular structures.[1] Diverse small molecular systems have been reported, which exhibit three conductivity states ("0", "1" and "2" states) in response to the applied voltage and meet the materials demands for the new-generation date-storage devices with faster speed, light weight, higher density, and lower power.[2] A popular design approach for small molecules involves the synthesis of large π-cores with multi electron-withdrawing groups (e. g. cyano, nitro, pyrazine) or/and multilevel stable oxidation states.[3] However, there is no obvious correlation between the number of conductivity states and the different electron-withdrawing groups or/and the multiplicity of oxidation states. Sometimes, memory devices based on small molecules with different electron-withdrawing groups or/and multilevel stable oxidation states exhibit only binary memory behavior instead of multiple states.[4] A better understanding of such correlation is very important.

Phenazine derivatives or azaacenes have received increasing attention due to their wide applications in organic electronic devices such as organic light emitting diodes, organic field-effect transistors, and organic solar cells.[5] More recently, phenazine derivatives, acting as electron-active layer, have been applied in memory devices as the presence of two imine nitrogen groups renders the aromatic system electron deficient, creating a potentially useful electron transporting material.[6] In this paper, we focused on how the film morphology changes can affect the memory performance based on phenazine derivatives because many properties of organic molecules are dependent on the film morphology.[7] To address this issue, two small molecules, 7,8-bis(decyloxy)-3-(2-hydroxy-4,5-dinitrophenoxy)phenazin-2-ol

(2OHPz) and 7,8-bis(decyloxy)-3-(2-(decyloxy)-4,5-dinitrophenoxy)phenazin-2-ol (1OHPz) (Scheme 1), were designed and synthesized with the same electron-withdrawing group (nitro and pyrazine) and molecule backone, but the different terminal substituted groups. We anticipate that the film morphology based on 2OHPz and 1OHPz are different because 2OHPz with two hydroxyl groups might induce the molecule ordered-organization while 1OHPz with one alkoxyly group might weaken intermolecular interaction. The morphologies of film are characterized by absorption spectra, XRD, and AFM. Furthermore, sandwich-structured memory devices based on 2OHPz and 1OHPz have been carefully investigated in details. We aim to achieve not only well-defined morphologies of the film, but also the tunable electronic properties of phenazine derivatives.

2 Experimental Section

2.1 Materials

10% Pd/C, 1,2-difluorobenzene, and hydrazine monohydrate were purchased from Alfa Aesar. 2,5-Dihydroxy-1,4-benzoquinone and 1-bromodecane were purchased from Sigma-Aldrich. 7,8-bis(decyloxy)phenazine-2,3-diol and 1,2-difluoro-4,5-dinitrobenzene were synthesized according to a literature procedure.[8] Other chemicals and solvents were used directly without further purification.

2.2 Characterization

Using CF_3COOD (TFA), $CDCl_3$, or DMSO-d_6 as solvents and tetramethylsilane (TMS) as the internal standard, ^{1}H NMR and ^{13}C NMR spectra were measured on a Bruker Advance 300 or 400 MHz NMR spectrometer at ambient temperature. UV/Vis absorption spectra were carried out at room temperature with a Shimadzu UV-3600 spectrophotometer. High resolution mass spectra (HRMS) were recorded on a Waters Q-Tof premierTM mass spectrometer. Thermogravimetric analysis (TGA) was carried out on a TA Instrument Q500 Thermogravimetric Analyzer at a heating rate of 10 ^{o}C min^{-1}. Cyclic voltammetry measurements were carried out on a CHI 604E electrochemical analyzer. Glassy carbon (diameter: 1.6 mm; area 0.02 cm^2) was used as a working electrode, platinum wires were used as counter electrode and reference electrode, respectively. Fc^+/Fc was used as an internal standard. Potentials were recorded versus Fc^+/Fc in a solution of anhydrous dichloromethane (DCM) with 0.1M tetrabutylammonium hexafluorophosphate ($TBAPF_6$) as a supporting electrolyte at a scan rate of 100 mV s^{-1}. Atomic force microscopy (AFM) measurements were performed using a MFP-3DTM (Digital Instruments/Asylum Research) AFM instrument. The as-prepared films were characterized by powder X-ray diffraction (XRD, Rigaku Ultima IV, Japan) with Cu Kα radiation source (λ = 0.154178 nm).

2.3 Fabrication of the memory devices

The indium-tin oxide (ITO) glass was pre-cleaned by sonicating for 15 min with deionized water, acetone and ethanol, sequentially. Then the small organic molecule was deposited onto the surface of the ITO under a pressure of 10^{-6} Torr. The thickness of the film was typically ~ 100 nm, which was traced by a calibrated quartz crystal monitor. Finally, aluminum (Al) was thermally evaporated onto the film surface at 5×10^{-6} Torr through a shadow mask to yield top electrodes with thickness around 120 nm and area of 0.0314 mm^2.

2.4 Synthesis

The synthetic procedure for the preparation of 2OHPz and 1OHPz is depicted in Scheme 1. The compounds were fully characterized using ^{1}H and ^{13}C NMR spectroscopy and mass spectrometry.

Scheme 1 Synthetic route of: (i) K_2CO_3, 1,2-difluoro-4,5-dinitrobenzene, DMF, N_2, 100 ^{o}C, 85 %; (ii) K_2CO_3, 1-bromodecane, DMF, N_2, 100 ^{o}C, 90 %.

Synthesis of 7,8-bis(decyloxy)-3-(2-hydroxy-4,5-dinitrophenoxy)phenazin-2-ol (2OHPz): A mixture of 7,8-bis(decyloxy)phenazine-2,3-diol (1.57 g, 3 mmol) and K_2CO_3 (2.07 g, 15 mmol) in 75 mL *N*,*N*-dimethylformamide (DMF) was stirred 2 h under N_2 atmosphere. 1,2-difluoro-4,5-dinitrobenzene (735 mg, 3.6 mmol) was added in 10 mL of DMF and the mixture was heated at 100 °C for 3 days. The mixture was allowed to cool down to ambient temperature before pouring into deionized water (500 mL). The obtained precipitate was isolated by filtration and washed with acetone and chloroform. Then, the red precipitate was dispersed in DMF and 2M HCl (10 mL) was added. The yellow-green powder 2OHPz (1.80 g, 2.6 mmol, yield: 85%) was isolated by filtration.

^{1}H NMR (400 MHz, TFA) δ 7.96 (s, 1H), 7.95 (s, 1H), 7.89 (s, 1H), 7.66 (s, 1H), 7.62 (s, 1H), 6.95 (s, 1H), 4.43 (t, *J* = 6.0 Hz, 4H), 2.04-1.99 (dd, *J* = 13.5, 6.3 Hz, 4H), 1.68 - 1.56 (m, 4H), 1.51 - 1.22 (m, 24H), 0.85 (t, *J* = 6.0 Hz, 6H). ^{13}C NMR (100 MHz, TFA) 160.68, 160.02, 153.90, 147.59, 147.01, 146.49, 137.52, 136.83, 133.21, 133.17, 132.72, 129.35, 107.57, 106.94, 106.16, 99.76, 98.96, 72.00, 71.89, 31.46, 29.05, 29.02, 28.85, 28.68, 27.84, 25.40, 22.01, 12.29. HR-MS, calcd for $C_{38}H_{51}O_9N_4$, 709.3597, found, 709.3773.

Synthesis of 7,8-bis(decyloxy)-3-(2-(decyloxy)-4,5-dinitrophenoxy)phenazin-2-ol (1OHPz): A mixture of 2OHPz (706 mg, 1 mmol) and K_2CO_3 (690 mg, 5 mmol) in 25 mL DMF was stirred 2 h under N_2 atmosphere. 1-bromodecane (663 mg, 3 mmol) was added in 5 mL of DMF and the mixture was heated at 100 °C for 24 h. The mixture was allowed to cool down to ambient temperature before pouring into deionized water (200 mL) and 2 M HCl (5 mL) was added. The obtained precipitate was isolated by filtration and washed with water and cool ethanol. The yellow-green powder 1OHPz (763 mg, 0.9 mmol, Yield: 90 %) was isolated by filtration.

^{1}H NMR (400 MHz, $CDCl_3$) δ 7.70 (s, 1H), 7.53 (s, 1H), 7.51 (s, 1H), 7.24 (s, 1H), 7.23 (s, 1H), 6.68 (s, 1H), 4.19 (t, *J* = 6.3 Hz, 4H), 4.05 (t, *J* = 6.4 Hz, 2H), 1.97 - 1.90 (m, 4H), 1.88 - 1.82 (m,

2H), 1.58 - 1.48 (m, 6H), 1.40 - 1.25 (m, 36H), 0.88 (t, J = 6.6 Hz, 9H). ^{13}C NMR (100 MHz, $CDCl_3$) δ 154.36, 154.30, 150.69, 145.07, 142.93, 142.49, 141.50, 141.30, 140.13, 139.66, 134.16, 133.15, 114.48, 112.22, 111.96, 105.32, 105.28, 102.72, 70.48, 69.29, 31.92, 31.89, 29.63, 29.58, 29.55, 29.53, 29.39, 29.36, 29.32, 29.29, 28.90, 28.76, 26.03, 25.83, 22.69, 14.11. HR-MS, calcd for $C_{48}H_{71}O_9N_4$, 847.5221, found, 847.5211.

3 Results and discussion

3.1 Photophysical, electrochemical, and thermal properties

The normalized optical absorption spectra of 2OHPz and 1OHPz in DCM solution are shown in Figure 1. The absorption spectrum of 2OHPz shows three prominent bands at 269, 398 and 421 nm, which can be ascribed to a localized aromatic π-π* transition and phenazine core, respectively. The absorption spectrum of 1OHPz is similar to that of 2OHPz since the molecular backbone is the same and changing the hydroxyl to alkoxyl group on the dinitrobenzene (not on the phenazine unit) does not affect the electronic properties. The absorption edges of 2OHPz and 1OHPz extend to ~ 450 and 440 nm, from which the optical band gaps (E_g^{opt}) are estimated to be 2.27 and 2.32 eV, respectively.

Cyclic voltammetry measurements of two compounds were performed in DCM solution (with 0.1 M $TBAPF_6$) to investigate the electrochemical properties. As shown in Figure 2, the onset oxidation potentials (E_{ox}^{onset}) of 2OHPz and 1OHPz are the same (1.47 V). The highest occupied molecular orbital (HOMO) energy levels of 2OHPz and 1OHPz were estimated to be -6.05 eV from the onset oxidation potential with reference to Fc^+/Fc (-4.8 eV) using the equation of $E_{HOMO} = -[4.8-E_{Fc} + E_{ox}^{onset}]$ eV. The lowest unoccupied molecular orbital (LUMO) energy levels of 2OHPz and 1OHPz are -3.78 and -3.73 eV according to the equation of $E_{LUMO} = E_{HOMO} + E_g^{opt}$.

Figure 1 Normalized optical absorption spectra at 421 nm of 2OHPz and 1OHPz in dilute DCM solution.

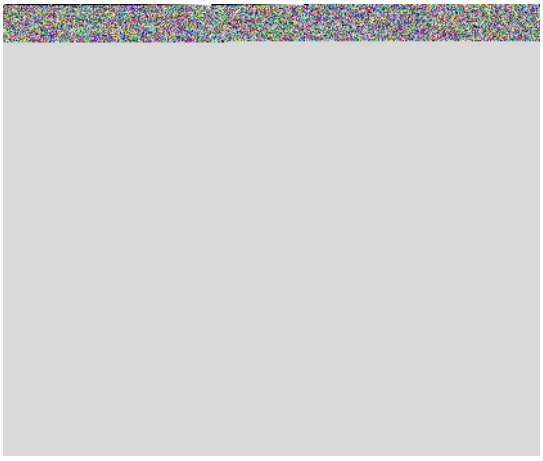

Figure 2 Cyclic voltammograms curves of 2OHPz and 1OHPz in DCM solution with $TBAPF_6$ (0.1 M) as the supporting electrolyte. The scan rate: 100 mV s^{-1}.

The thermal properties of 2OHPz and 1OHPz were evaluated by TGA under nitrogen atmosphere. As shown in Figure S7, 2OHPz and 1OHPz exhibit very good thermal stability with an onset decomposition temperature of ~ 281 and 347 ^oC (considering the 5% weight loss temperature).

3.2 Current-voltage (*I-V*) characteristics of the memory devices

The typical I-V curves of the memory device based on ITO/2OHPz or 1OHPz/Al sandwich structure are shown in Figure 3. In the case of 2OHPz, the current increased slowly with the applied negative voltage sweep while the current level remained low, indicating that the memory device was initially at the low-conductivity state (OFF, "0"). A sharp transition from the OFF ("0") state to the intermediate-conductivity (ON1, "1") was observed at switching threshold voltage (STV) of -1.80 V with increased negative voltage. When the negative voltage continued to increase, the current level boosted abruptly to 10^{-1} A (ON2, "2") at -3.62 V (sweep 1). The transitions from OFF-to-ON1 and then ON1-to-ON2 can be regarded as a "writing" process. The memory device could not erase and remained at the ON2 state when the negative sweep was repeated (sweep 2), indicating the nonvolatile write-once read-many-times (WORM) characteristics for the memory device. Another cell of the memory device was measured over a voltage range from 0 to -3 V (sweep 3) and an abrupt increase in current density was observed at STV of -1.81 V, indicating the transition from the OFF state to ON1 state. The memory device remained at ON1 state in the next sweep from 0 to -3 V (sweep 4). In sweep 5 from 0 to -6 V, the cell underwent a transition from ON1 state to ON2 state at -3.73 V. Once it was switched to ON2 state, the memory device cannot return to both ON1 state and OFF state (sweep 6). The distinctive OFF, ON1, and ON2 states (i.e., different responses to external electric field) can be programmed to correspond to "0", "1", and "2" signals, respectively, suggesting the device's potential application for ternary data storage. These three states of the ternary memory cell are distinct and the current ratio of "OFF", "ON1", and "ON2" states is 1: 10^3: $10^{8.8}$. For the ITO/1OHPz /Al device, its $I - V$ curves distinctively exhibited two bistable conductivity states. During the first sweep from 0 to -6 V, an abrupt increase in the

current level was observed from 10^{-9} A to 10^{-1} A at STV of -3.0 V, indicating the transition from the OFF state to ON state. The memory device remained at the ON state when the negative sweep was repeated (sweep 2) or the reverse voltage sweep (sweep 3), indicating the nonvolatile WORM characteristic for the memory device. Figure S8 shows the retention times of the two memory devices for the OFF, ON1, and ON2 or OFF and ON states. Under a constant stress of −1 V, no significant degradation in current for all different states could be observed for at least 10 000 s during the readout test, indicating that the memory performance is stable.

Figure 3 I-V characteristics of the memory devices (ITO/2OHPz/Al and ITO/1OHPz/Al, respectively) fabricated with (a) 2OHPz or (b) 1OHPz.

3.3 Proposed memory mechanisms

To gain further insights into the different memory behaviour of 2OHPz and 1OHPz, AFM, X-ray diffraction (XRD), UV-vis absorption and theoretical calculations (using the density functional theory (DFT) with generalized gradient approximation (GGA), which is implemented in DMol3 code) were carried out. As shown in Figure 4, the AFM height image of the 2OHPz film thermally evaporated onto the ITO surface indicates the formation of self-organized fibril structures, which is in sharp contrast to that of the 1OHPz film. This variation suggests different degrees of aggregation in these films, which is also in accordance with the XRD and UV-vis absorption results. As shown in Figure 5, there is one diffraction peak at 2^{-} 16.11^{o} for the film of 2OHPz, indicating the formation of more ordered structure in the thin film. In contrast, there is no obvious diffraction peak in the film of 1OHPz. The UV-vis spectroscopic studies reveal very similar absorption features in the DCM solutions of 2OHPz and 1OHPz. In the thin films, the absorptions at the longest wavelength are both blue-shifted compared to these from the DCM solution, however the peak position of 2OHPz is blue-shifted ～ 10 nm more than that of 1OHPz film (Figure S9). These phenomena suggest that 2OHPz molecules pack more orderly than 1OHPz in the thin film. As shown in Figure 6, the dihedral angles between phenazine ring and dinitrobenzene group are the similar. In addition, the spatial distributions of the HOMO and LUMO levels of 2OHPz and 1OHPz are calculated. The electron density distributions of the HOMO for 2OHPz mainly locate on phenazine ring while the LUMO is mainly distributed on dinitrobenzene group. Thus, a charge-transfer (CT) interaction can occur between the electron donor moieties and the electron acceptor moieties. The results of calculation of 1OHPz are the similar to that of 2OHPz. The electrostatic surface potential (ESP) plots of 2OHPz (Figure 6) and 1OHPz (Figure 6) show that an open channel is formed from the molecular surface of 2OHPz and 1OHPz along the molecular backbone with continuous positive electrostatic potential (in red), through which charge carriers can migrate. However, there are also some regions with negative electrostatic potential (in blue), which arise from the electron-accepting groups, such as nitro and pyrazine groups. These negative regions can serve as ‘‘charge traps’’ to block the transporting of charge carriers. As shown in Figure 7, the energy barrier between the work functions of Al and LUMO of 2OHPz or 1OHPz is lower than the energy barrier between the work function of ITO and HOMO, suggesting that electron injection from Al into the LUMO of 2OHPz or 1OHPz is a favored process. Under the applied low voltage, electrons are injected from Al into the 2OHPz thin film, and the subsequent transporting is blocked by the nitro and pyrazine groups. As a result, the memory device exhibits a low-conductivity state and the current increases slowly. At the elevated voltage, the increased number of charge carriers is enough to fill the traps from the nitro groups, leading to better conductivity and an intermediate-conductivity (ON1) state. However, not all the traps are filled at this state - only these traps from the more electron-deficient nitro groups are filled, leaving alone these from the weaker pyrazine acceptor. When the bias is further increased, the traps from pyrazine group are eventually filled, which leads to the current transition from the ON1 to ON2 state. Therefore, the memory device based on ITO/2OHPz/Al shows ternary memory characteristics. The memory behavior of 1OHPz is similar to that of 2OHPz at low voltage, but differs significantly at increased voltage, which could be accounted for by the difference in intermolecular interactions. In both cases, charge carriers can move both intramolecularly and intermolecularly after being injected into the organic thin films. As for the memory device based on ITO/2OHPz/Al, charge carriers can migrate relatively easily among the adjacent molecules due to the orderly intermolecular packing. Under such circumstances, the gradient of the electron accepting abilities of nitro and pyrazine groups could be resolved, resulting in sequential opening of the conduction channels and thus two conductive ON states. In the case of ITO/1OHPz/Al devices, transport of charge carriers, mostly governed by electron hopping in between molecules, is

much less efficient than 2OHP due to unfavored intermolecular packing. As a result, the injected charge carriers have to fill all the traps of one molecule before migrating to the next molecule, thus no differentiation between the two different trapping groups and only binary memory characteristics is observed.

Figure 4 AFM height images of (a) 2OHPz and (b) 1OHPz thin films on ITO glass substrates.

Figure 5 XRD spectra of 2OHPz and 1OHPz thin films on ITO glass substrates.

Figure 6 Optimized ground-state geometry (OG-Sg) of 2OHPz and 1OHPz with B3LYP/6-31G* in the gas phase; calculated spatial distributions of the HOMO and LUMO levels; ESP surface plot of 2OHPz and 1OHPz.

Figure 7 Energy level diagram of HOMO and LUMO for 2OHPz and 1OHPz along with the work function of Al and ITO.

4 Conclusion

In summary, we have successfully synthesized two phenazine derivatives, 2OHPz and 1OHPz, with the same electron-withdrawing groups (nitro and pyrazine) and molecular backbone, but different terminal groups. The sandwich-structured memory devices based on ITO/2OHPz/Al exhibited excellent ternary memory behavior with high ON2/ON1/OFF current ratios of $10^{8.8}/10^{3}/1$ at switching threshold voltages of -1.80 V/-3.62 V. The sandwich-structure memory devices based on ITO/1OHPz/Al displayed binary memory behavior with ON/OFF current ratios of $10^{7.5}/1$ at a switching threshold voltage of -3.0 V. The different memory behavior is attributed to the different molecular packing in the two phenazine derivatives, which is confirmed by AFM, XRD and UV-vis absorption. Our findings could provide guidance for the design and synthesis of new heteroacenes as promising materials candidates for multi-state memory devices.

Acknowledgements

P.-Y. Gu thanks Ms Tan Si Yu and Prof Yanli Zhao for helping us test the HRMS. Q.Z. acknowledges financial support from AcRF Tier 1 (RG 16/12) and Tier 2 (ARC 20/12 and ARC 2/13) from MOE, and the CREATE program (Nanomaterials for Energy and Water Management) from NRF.

Notes and references

[1] *School of Materials Science and Engineering, Nanyang Technological University, Singapore 639798, Singapore.*
** Correspondence to Q. Zhang, E-mail: qczhang@ntu.edu.sg*
[2]*College of Chemistry, Chemical Engineering and Materials Science, Soochow University, Suzhou, 215123, China.*
** Correspondence to J.-M. Lu or Q. -F. Xu, E-mail: lujm@suda.edu.cn; xuqingfeng@suda.edu.cn*
[3]*The Molecular Foundry and ‡Advanced Light Source, Lawrence Berkeley National Laboratory, One Cyclotron Road, Berkeley, California 94720, United States*
[4]*Division of Chemistry and Biological Chemistry, School of Physical and Mathematical Sciences, Nanyang Technological University, Singapore 637371, Singapore*

† Electronic Supplementary Information (ESI) available: [details of experimental section]. See DOI: 10.1039/b000000x/

1 a) J. Fang, H. You, J. Chen, J. Lin, and D. Ma, *Inorg. Chem.*, 2006, **45**, 3701; b) F. Zhao, J. Liu, X. Huang, X. Zou, G. Lu, P. Sun, S. Wu, W. Ai, M. Yi, X. Qi, L. Xie, J. Wang, H. Zhang and W. Huang, *ACS Nano*, 2012, **6**, 3027; c) J. Xiao, Z. Yin, Y. Wu, J. Guo, Y. Cheng, H. Li, Y. Z. Huang, Q. Zhang, J. Ma, F. Boey, H. Zhang, and Q. C. Zhang, *Small*, 2011, **7**, 1242; d) G. Liu, Q.-D. Ling, E. Y. H. Teo, C.-X. Zhu, D. S.-H. Chan, K.-G. Neoh and E.-T. Kang, *ACS Nano*, 2009, **3**, 1929; e) J. Xiao, Z. Yin, H. Li, Q. Zhang, F. Boey, H. Zhang and Q. C. Zhang, *J. Am. Chem. Soc.* 2010, **132**, 6926; f) C. Simão, M. Mas-Torrent, J. Casado-Montenegro, F. Otón, J. Veciana, C. Rovira, *J. Am. Chem. Soc.*, 2011, **133**, 13256; g) E. Kapetanakis, A. M. Douvas, D. Velessiotis, E. Makarona, P. Argitis, N. Glezos and P. Normand, *Adv. Mater.*, 2008, **20**, 4568; h) C. W. Chu, J. Ouyang, J.-H. Tseng and Y. Yang, *Adv. Mater.*, 2005, **17**, 1440; i) R. J. Tseng, J. Huang, J. Ouyang, R. B. Kaner and Yang, *Nano Lett.*, 2005, **5**, 1077; j) J. Ouyang, C.-W. Chu, C. R. Szmanda, L. Ma and Y. Yang, *Nat. Mater.*, 2004, **3**, 918; k) L. D. Bozano, B. W. Kean, M. Beinhoff, K. R. Carter, P. M. Rice and J. C. Scott, *Adv. Funct. Mater.*, 2005, **15**, 1933; l) B. Hu, C. Wang, J. Wang, J. Gao, K. Wang, J. Wu, G. Zhang, W. Cheng, B. Venkateswarlu, M. Wang, P. S. Lee, and Q. Zhang, *Chem. Sci.*, 2014, **5**, 3404.

2 a) A. J. Kronemeijer, H. B. Akkerman, T.Kudernac, B. J. van Wees, B. L. Feringa, P. W. M. Blom and B. de Boer, *Adv. Mater.*, 2008, **20**, 1467; b) G. Li, K. Zheng, C. Wang, K. S. Leck, F. Hu, X. W. Sun, and Q. Zhang, *ACS Appl. Mater. interface* 2013, **5**, 6458; c) J. Wang and G. D. Stucky, *Adv. Funct. Mater.*, 2004, **14**, 409; d) T. Lee, S.-U. Kim, J. Min and J. -W Choi, *Adv. Mater.*, 2010, **22**, 510; e) P. Y. Gu, F. Zhou, J. Gao, G. Li, C. Wang, Q. F. Xu, Q. Zhang and J. M. Lu, *J. Am. Chem. Soc.*, 2013, **135**, 14086.

3 a) J.-S. Lee, Y.-M. Kim, J.-H. Kwon, J. S. Sim, H. Shin, B.-H. Sohn and Q. Jia, *Adv. Mater.*, 2011, **23**, 2064; b) S.-J. Liu, P. Wang, Q. Zhao, H.-Y. Yang, J. Wong, H.-B Sun, X.-C. Dong, W.-P. Lin and W. Huang, *Adv. Mater.*, 2012, **24**, 2901; c) C. Ye, Q. Peng, M. Li, J. Luo, Z. Tang, J. Pei, J. Chen, Z. Shuai, L. Jiang and Y. Song, *J. Am. Chem. Soc.*, 2012, **134**, 20053; d) C. Wang, B. Hu, J. Wang, J. Gao, G. Li, W.-W. Xiong, B. Zou, M. Suzuki, N. Aratani, H. Yamada, F. Huo, P. S. Lee, and Q. Zhang, *Chem. Asian J.* 2015, **10**, 116.

4 H. Liu, H. Zhuang, H. Li, J. Lu and L. Wang, *Phys. Chem. Chem. Phys.*, 2014, **16**, 17125.

5 a) G. J. Richards, J. P. Hill, T. Mori and K. Ariga, *Org. Biomol. Chem.*, 2011, **9**, 5005; b) Z. Liang, Q. Tang, J. Xu and Q. Miao, *Adv. Mater.*, 2011, **23**, 1535; c). X. Xu, G. Yu, S. Chen, C. A. Di and Y. Liu, *J. Mater. Chem.*, 2008, **18**, 299. d) C. Fu, M. Li, Z. Su, Z. Hong, W. Li and B. Li, *Appl. Phys. Lett.*, 2006, **88**, 093507.

6 C. Wang, J. Wang, P. Z. Li, J. Gao, S. Y. Tan, W. W. Xiong, B. Hu, P. S. Lee, Y. Zhao and Q. Zhang, *Chem. Asian J.*, 2014, **9**, 779.

7 a) Q. Y. Yang and J. M. Lehn, *Angewandte Chemie*, 2014, **53**, 4572; b) X. Cheng, D. Li, Z. Zhang, H. Zhang and Y. Wang, *Org. Lett.*, 2014, **16**, 880; c) Y. Chen, G. Liu, C. Wang, W. Zhang, R.-W. Li and L. Wang, *Mater. Horiz.*, 2014, **1**, 489; d) X.-D. Zhuang, Y. Chen, G. Liu, B. Zhang, K.-G. Neoh, E.-T. Kang, C.-X. Zhu, Y.-X. Li and L.-J. Niu, *Adv. Funct. Mater.*, 2010, **20**, 2916.

8 P.-Y. Gu, J. Gao, C.-J. Lu, W. Chen, C. Wang, G. Li, F. Zhou, Q.-F. Xu, J.-M. Lu and Q. Zhang, *Mater. Horiz.*, 2014, **1**, 446.

Substituent groups effect on the morphology and memory performance of phenazine derivatives

Pei-Yang Gu, Yong Ma, Jing-Hui He, Guankui Long, Chengyuan Wang, Wangqiao Chen, Yi Liu, Qing-Feng Xu, Jian-Mei Lu, and Qichun Zhang

The memory devices based on ITO/2OHPz/Al exhibited excellent ternary memory behavior while devices based on ITO/1OHPz/Al displayed binary memory behavior.